Geotechnical Testing Journal

doi:10.1520/GTJ20170443 / Vol. 43 / No. 3 / 2020 / available online at www.astm.org

Filip Stanić,[1,2] Yu-Jun Cui,[1] Pierre Delage,[3] Emmanuel De Laure,[1] Pierre-Antoine Versini,[2] Daniel Schertzer,[2] and Ioulia Tchiguirinskaia[2]

A Device for the Simultaneous Determination of the Water Retention Properties and the Hydraulic Conductivity Function of an Unsaturated Coarse Material; Application to a Green-Roof Volcanic Substrate

Reference

F. Stanić, Y.-J. Cui, P. Delage, E. De Laure, P.-A. Versini, D. Schertzer, and I. Tchiguirinskaia, "A Device for the Simultaneous Determination of the Water Retention Properties and the Hydraulic Conductivity Function of an Unsaturated Coarse Material; Application to a Green-Roof Volcanic Substrate," *Geotechnical Testing Journal* 43, no. 3 (May/June 2020): 547–564. https://doi.org/10.1520/GTJ20170443

ABSTRACT

The determination of the water retention curve (WRC) and hydraulic conductivity function (HCF) of a specific volcanic coarse granular material used as a substrate for urban green roofs in Europe was carried out on a newly developed specific device in which low suctions, typical of coarse granular materials, were controlled. Smaller suctions (up to 32 kPa) were imposed by using a hanging column system, and larger suctions (between 32 and 50 kPa) were imposed by using the axis translation technique in the same cell. The changes in suction during the tests were monitored by using a high accuracy differential pressure transducer. They were also used to determine the HCF by means of both Kunze and Kirkham's and Gardner's methods. The former technique was used at low suctions (<4 kPa) to account for the impedance effects due to the high air entry value ceramic porous disk and the latter was used between 4 and 50 kPa. Good comparability was observed in the data from both methods, demonstrating the good performance of the device. The mathematical expressions of the WRC of van Genuchten and Brooks and Corey were used, and a good fitting with our experimental data was obtained. Conversely, the HCFs derived from these expressions appeared to lead to a significant underestimation, confirming the need of an operational and simple device for the experimental determination of the HCF. Also, this material proved to be an appropriate material for green urban infrastructures, because of its lightweight, satisfactory water retention capability and hydraulic conductivity.

Manuscript received December 5, 2017; accepted for publication April 19, 2019; published online June 26, 2019. Issue published May 1, 2020.

[1] Ecole des Ponts ParisTech, Navier/CERMES, 6-8 av. Blaise Pascal, Cité Descartes, Champs-sur-Marne, Marne-la-Vallée 77455 Cedex 2, France, https://orcid.org/0000-0003-0271-5993 (F.S.)

[2] Ecole des Ponts ParisTech, HM&Co, 6-8 av. Blaise Pascal, Champs-sur-Marne, Marne-la-Vallée 77455 Cedex 2, France

[3] Ecole des Ponts ParisTech, Navier/CERMES, 6-8 av. Blaise Pascal, Cité Descartes, Champs-sur-Marne, Marne-la-Vallée 77455 Cedex 2, France (Corresponding author), e-mail: pierre.delage@enpc.fr, https://orcid.org/0000-0002-2101-5522

Copyright © 2019 by ASTM International, 100 Barr Harbor Drive, PO Box C700, West Conshohocken, PA 19428-2959

Keywords

green-roof material, water retention, hydraulic conductivity, hanging column, axis translation, Gardner's method, Kunze and Kirkham's method

Introduction

Within the context of global warming, green roofs are considered an efficient option to reduce the urban heat island effect that characterizes large contemporary urban concentrations, thanks to the evapotranspiration of the vegetal (lawn or trees) grown on them. Green roofs are also interesting to reduce urban runoff. The substrates used in green roofs have to be light enough and present satisfactory water retention and transfer properties. Coarse volcanic granular substrates appear to be relevant in this context and they are frequently used in green roofs, like for instance in the case of the "Green Wave" of the Bienvenüe building (Versini et al. 2018) located close to Ecole des Ponts ParisTech in the Descartes campus of Marne-la-Vallée, 18 km east of Paris (see **fig. 1**). The green roof is covering three waves or 260 m long and 80 m wide, on which a 20 cm–thick layer of substrate has been placed.

The use of substrates in urban green roofs appears to be rather empirical to date, and very few data on their water retention and transfer properties are available. Also, whereas many investigations have been devoted to the determination of the water retention properties of unsaturated soils, much fewer data address their transfer properties because of the technical difficulties met in their experimental determination. This is even truer in the case of coarse materials like the volcanic substrate considered here.

To cope with these limitations, the article describes the development of a specific controlled suction device for coarse granular materials, based on both a tensiometry principle (through the hanging column technique) and the axis translation method. The device is used to determine the water retention properties of the volcanic substrate used in the "Green Wave." The device is also used for a simultaneous determination of the change in hydraulic conductivity of the unsaturated substrate along a drying path by means of Gardner's (1956) and Kunze and Kirkham's (1962) methods, with special care devoted to impedance effects. The experimental data obtained are compared to those derived from the water retention curves (WRCs) through Mualem's (1976) approach so as to check the validity, for the coarse material investigated in this work, of some models that are often used in the literature.

Material and Methods

MATERIAL

The "Green Wave" roof of the Bienvenüe building is presented in **figure 1**. The VulkaTec volcanic material (VulkaTec Riebensahm GmbH 2016) is presented in the photo of **figure 2**, and its main characteristics are

FIG. 1

The "Green Wave" of the Bienvenüe building located close to Ecole des Ponts ParisTech, Marne la Vallée.

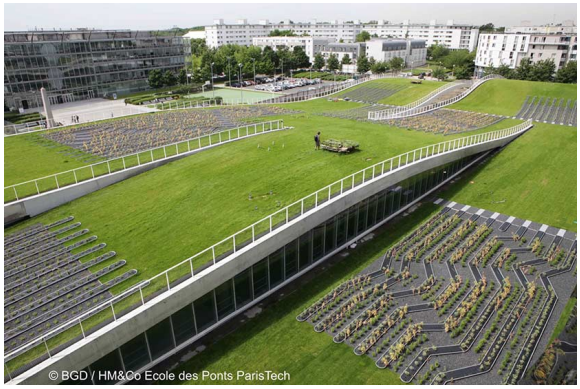

FIG. 2

Photo of the volcanic substrate used for the "Green Wave."

presented in Table 1. The grain density was determined by using a water pycnometer, providing an average value of 2.35 Mg/m^3, a small value compatible with the volcanic origin of the material. The dry density of the specimen tested was determined by calculating its volume (from its dimensions) and measuring its weight, providing a value of 1.42 Mg/m^3, light enough not to load the roof significantly. The resulting porosity was found equal to 0.395. A percentage of 4 % of organic matter was determined by using the French standard AFNOR 1998, which consists of comparing the specimen weight before and after heating during at least 3 hours at a temperature between 450°C and 500°C. The grain size distribution curve of the substrate, determined by sieving following the French standard AFNOR 1996, is presented in figure 3 (solid line). The distribution of fine particles (<80 µm) was obtained by sedimentation according to the French standard AFNOR 1992. It can be noticed that 50 % of the grains are larger than 1.6 mm with 10 % of particles between 10 and 20 mm in the coarse range and 13 % of fine particles smaller than 80 µm. Also represented in figure 3 (dashed curve) is the grain size distribution curve of the material used for the test, with all particles smaller than 6 mm. Particles larger than 6 mm were discarded because we used

TABLE 1

Basic characteristics of "Green Wave" substrate

Density of the Grains	Dry Density	Porosity	Curvature Coefficient	Uniformity Coefficient	Percentage of Organic Matter
ρ_s, Mg/m^3	ρ_d, Mg/m^3	φ, -	C_c, -	C_u, -	C_{MOC}, %
2.35	1.42	0.395	1.95	55	4

FIG. 3

Grain size distribution curve of the volcanic substrate.

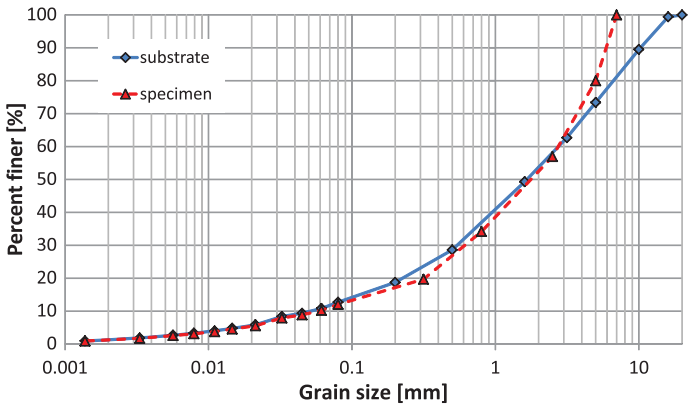

a 70-mm diameter cell. For the same volume, a specimen with large particles discarded will contain more small particles, resulting in a larger porosity, more water retained at a given suction, and larger hydraulic conductivity. Given that the proportion of the coarse particles discarded is 20 %, a rough estimation of the overestimation could be between 10 % and 20 %. Also presented in **Table 1** are the curvature coefficient C_c ($C_c = (D_{30})^2/(D_{60} \times D_{10}) = 1.95$) and uniformity coefficient C_u ($C_u = D_{60}/D_{10} = 55$). According to ASTM D2487-06, *Standard Practice for Classification of Soils for Engineering Purposes (Unified Soil Classification System)* (2006), the material can be regarded as well graded.

METHODS OF CONTROLLING SUCTION

The various methods of controlling suction in soils include the hanging column technique (Buckingham 1907), axis translation technique (Richards 1941, 1947), osmotic technique (Zur 1966), and vapor equilibrium technique (Esteban 1990). A detailed description of these techniques and their adaptation in geotechnical testing can be found in Delage (n.d.); Vanapalli, Nicotera, and Sharma (2008); Blatz, Cui, and Oldecop (2008); Delage and Cui (2008); and Fredlund, Rahardjo, and Fredlund (2012).

Given that the volcanic substrate investigated here is granular with rather large grain sizes (see **fig. 2**), it was initially decided to use the hanging column technique because of its simplicity in use and its good accuracy in both the control of low suctions and measurement of water exchanges. However, we realized during the preliminary tests that at the largest height imposed in the hanging column technique ($h_k = 3.2$ m, corresponding to a suction of $s = 32$ kPa), a significant amount of water still remained in the substrate. It was then decided to impose larger suctions by using the axis translation technique. Note that the hanging column technique was kept at very low suctions because of its robustness and high accuracy in this range, in which a high-precision air pressure regulator would have been required if using the axis translation method.

In both cases, tests were conducted on a 24-mm high specimen placed into a metal 70-mm diameter cylindrical cell in contact at its bottom with a 50-kPa air entry value ceramic porous disk. A thin metal disk (5 mm thick) was placed on top of the specimen, so as to monitor changes in height by means of a displacement sensor (Mitutoyo Brand).

The Hanging Column Technique

The implementation of the hanging column technique is presented in **figure 4**. The cell is connected at its base through Valve V2 to an outlet controlled by Valve V3 and a water reservoir through Valve V1. The cell is also connected through a central tube to a mobile device that allows the imposition of water levels lower than that of the specimen, so as to apply suctions defined by the difference in water level between the specimen and mobile part (up to 32 kPa at the maximum height of 3.2 m).

The mobile device contains a smaller inner glass tube of $d_{inn} = 0.5$ cm and larger outer glass tube of diameter $d_{out} = 1.5$ cm. The inner tube is connected to the specimen while the differential pressure transducer is connecting the outer tube with the reference glass tube (see **fig. 4**). This pressure transducer (0.1 mm accuracy in water height) is able to provide high-frequency measurements that are necessary for the determination of the hydraulic conductivity function (HCF). A monitoring rate of 10 s was adopted, chosen small enough to capture the change in the capillary potential at small times through the change of the water level in the mobile device. This change is detected as the height difference between the water levels either in the inner (Valve V4 opened) or outer tube (Valve V5 opened) and the water level in the reference tube used to indicate a constant reference water level. Most tubes used in the setup are semi-rigid tubes made up of polyamide, except those used in the mobile device (inner and outer tubes) and reference tube, which are made up of glass.

The determination of the WRC along the drying path was carried out as follows:

Saturating the Whole System

Before starting, all of the system has to be saturated, particularly the tubes connected to the differential pressure transducer, because air bubbles in the tubes can result in misleading data. Saturation was done by placing the

FIG. 4

General layout of the hanging column system.

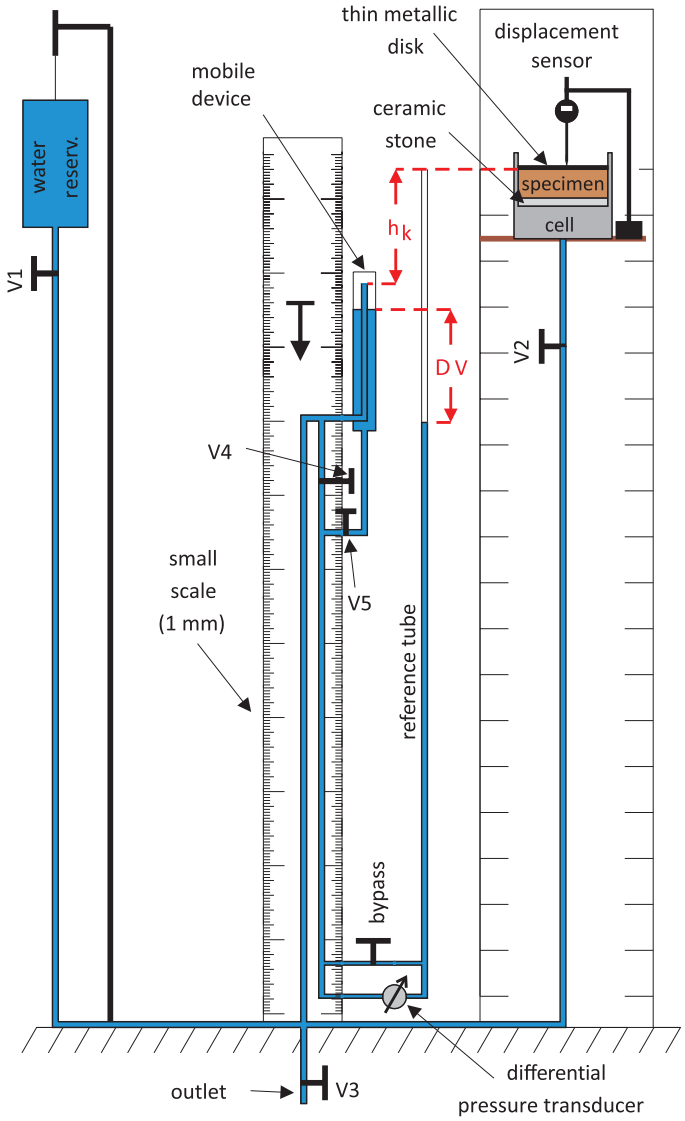

reservoir filled with demineralized de-aired water above the specimen (see fig. 4) and opening Valves V1 and V2 to let water infiltrate the specimen from the bottom to the top. Circulation of the water within the specimen was let over one night, resulting in having a water layer laying above the specimen.

To determine the degree of saturation after infiltration and water circulation, a specific test was carried out on a specimen of same density with the top face coinciding with the top of the cell, allowing for water overflow. Eight pore volumes of water were circulated through the specimen by means of a graduated water column that was connected at the specimen bottom. The specimen was weighed after water circulation, and the volume of water could be calculated, knowing also the dry weight of the specimen that was measured before the test. The test provided a degree of saturation of 98 %, which was found reasonably close to saturation. The 2 % remaining was probably due to the difficulty of fully saturating the small pores existing within the fine fraction (13 % < 80 μm). As in standard triaxial testing, full saturation could ideally be obtained by imposing a water back-pressure, which was not feasible in the present device.

Once saturation was completed, the water layer above the specimen was removed, and Valves V1 and V2 were closed. Prior to running the test, the mobile device was placed in such a position that the top of the inner tube

full of water was at the same level as the top of the specimen, resulting in $h_k = 0$ (see fig. 4). In order to check whether equilibrium was ensured, Valve V2 (see fig. 4) was opened. If there was no water movement in the inner tube, the experiment could start. Otherwise, the saturation procedure was repeated.

Imposing Suction

Two methods were used, according to the value of suction imposed.

(i) At smaller suctions, starting from saturation, it was observed that suction increases mobilized a significant volume of extracted water. Suction was then imposed by closing Valves V2 and V5, by filling the inner tube up to the top and moving down the mobile device at a position corresponding to the required suction. The water levels in the reference and outer tubes were carefully adjusted at the starting level in both tubes (see fig. 5A). The imposed suction was defined by the difference in height between the top of the specimen and the water level at the top of the inner tube (h_k in fig. 4). Valves V2 and V5 were then opened, resulting in water being extracted from the specimen under the effect of increased suction. The extracted volume of water (ΔV in fig. 4) flows from the top of the inner tube into the outer tube. It is monitored by the differential pressure transducer that measures the height difference between the water levels in the outer and reference tubes (ΔH_1—fig. 5A). Once equilibrium is reached (after 6–24 hours), a point on the WRC is obtained from the pair of values (θ_i, $h_{k,i}$) from the following equation:

$$\theta_i = \theta_{i-1} - \Delta V_i / V_{specimen,(i-\frac{1}{2})} \quad (1)$$

where ΔV_i is the volume of water [L^3] extracted from the specimen, $V_{specimen,(i-\frac{1}{2})}$, the average specimen volume [L^3] between the end and the start of the test, determined from the monitored changes in height of the specimen, and

FIG. 5

Description of the two procedures used: (*A*) change in water level observed in outer tube ($\Delta H1$) with Valve V4 closed and Valve 5 opened; and (*B*) change in water level observed in the inner tube ($\Delta H2$) with Valve 4 opened and Valve 5 closed.

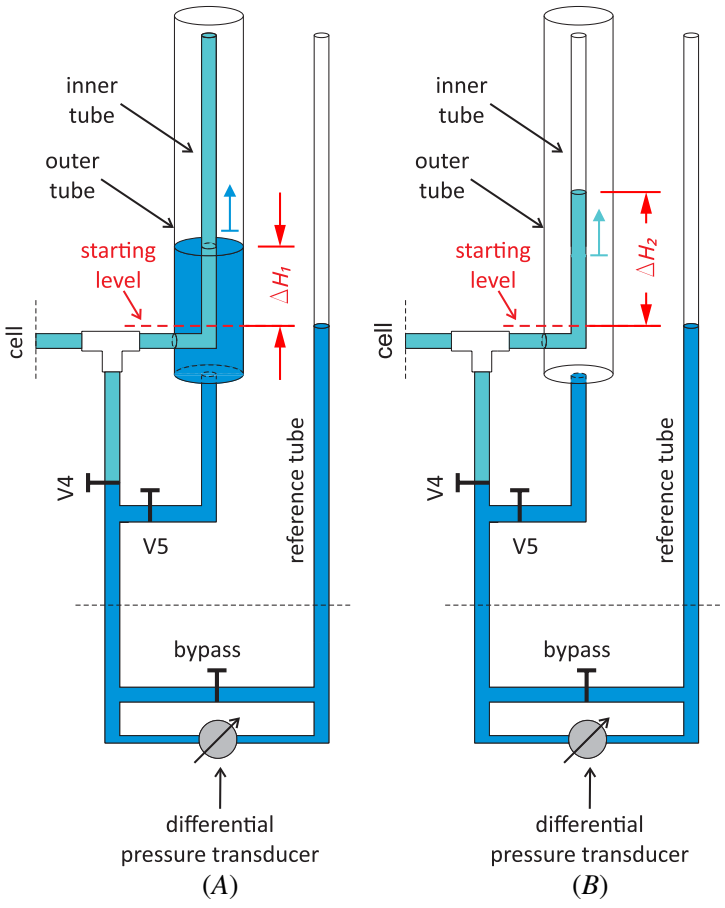

$(\theta_i - \theta_{i-1})$, the difference in volumetric water content [-] between the end and the start of the test. Note, however, that the monitoring of the changes in specimen height during the tests indicated very small changes, smaller than 0.5 mm (2 %), along the whole test, made up of 13-step increases in suction. The changes in height during each step were hence neglected.

(ii) At larger suctions, the quantity of extracted water appeared to be much smaller and the procedure was changed to improve accuracy. The initial water level in the inner tube was no longer imposed at its top but adjusted (by means of Valve V3) at a lower level, in such a way that overflow was avoided during water extraction from the specimen. The changes in height in the inner tube were then directly measured by the differential pressure transducer by closing Valve V5 and opening Valve V4. The imposed suction was calculated at the end of the measurement from the difference in height between the final water level in the inner tube and the top of the specimen (ΔH_2—**fig. 5*B***).

Before each new suction step, water levels in the outer (i) / inner (ii) and reference tubes were adjusted to the same level by opening the bypass valve (see **fig. 4**) in order to reset the differential pressure transducer. Water levels in the outer (i) / inner (ii) and reference tubes were then set to the required initial levels by carefully using Valve V3 in order to eliminate extra water through the outlet.

In this study, only the drying path was considered. But the apparatus can also be used along wetting paths, along the following steps:

(W1) Setting the initial position: the initial position of the mobile part is at the lowest vertical level, i.e., the final position at highest suction reached during the drying path. The specimen is hence capable of storing more water; thus a higher change in water level is expected. The water level change is recorded in the outer tube while the inner tube is filled up with water to the top and no longer used during the test. Initial water levels in the outer and reference tubes should be set at the top of the inner tube by opening Valves V1 and V4 and the bypass and letting water flow over the top of the inner tube. After reaching the required position, all valves and bypass should be closed.

(W2) Imposing suction: by opening Valves V5 and V2, water from the outer tube enters the specimen. The resulting decrease in water level in the outer tube is captured by the differential pressure transducer.

(W3) Reaching equilibrium: once equilibrium is reached, suction is calculated as the height difference between the water level in the outer tube and the top of the specimen. The corresponding water content is calculated like during the drying path but with an opposite sign, because water content is now increasing after each measurement $(\theta_i = \theta_{i-1} + \Delta V_i / V_{\text{specimen},(i-\frac{1}{2})})$.

(W4) Decreasing suction: to impose a lower suction, the mobile device is elevated; the outer and reference tubes are filled again, as described in Step W1; and the W2 procedure is repeated. When a smaller change in water level in the outer tube is expected (lower suctions, higher water content), the inner tube should be used by closing Valve V5 and using Valve V4, unlike in Step W2.

(W5) Final state of the wetting path: in order to bring back the specimen to zero suction, the mobile device should be located at the initial position of the drying path with the water levels in the inner and reference tubes corresponding to the specimen top. In case of a difference in height between the level in the inner tube and the top of the specimen (if h_k marked in **fig. 4** is higher than zero) after reaching equilibrium, the tubes should be refilled with water by opening Valves V1 and V4 and the bypass. After closing Valve V1 and the bypass and opening Valve V2 without changing the vertical position of the mobile device, no water movement in the inner tube should occur. If this is not the case, it means that zero suction was not obtained and the refilling procedure should be repeated.

As commented earlier, for determining the drying path the hanging column technique was used for heights up to 3.2 m corresponding to a maximum suction of 32 kPa. For higher suctions, the axis translation technique was applied.

The Axis Translation Technique

The axis translation technique was carried out by applying increasing air pressure on the top specimen surface. To do so, a cap connected to the air pressure supply source was placed on the top of the cell. Tests were carried out while keeping the specimen and mobile device at the same level above the differential manometer in order to

monitor the changes in height difference. The imposed suction was calculated as the difference between the air pressure applied on the specimen's upper surface and the change of water level inside the inner tube.

Before each test, the water level in the inner tube should be put at the same level as the top of the specimen, and some space should be left above the water level to allow for some level increase with no overflow during the measurement. Once the air pressure is imposed, Valves V2 and V6 are simultaneously opened, resulting in an increase of the water level in the inner tube until stabilization at equilibrium. The final suction is calculated as the difference between the applied air pressure and pressure corresponding to the water level increment in the inner tube, captured by the pressure transducer. The corresponding water content is calculated by using equation (1). This methodology was applied for suctions up to 50 kPa, the air entry value of the ceramic disk used. Higher suctions could be obtained with higher pressure and a ceramic disk of higher air entry value.

DETERMINATION OF THE HCF

Saturated State

The investigation on the HCF of the material started with the determination of the saturated one. To do so, the cell containing the specimen was disconnected from the device and connected to a Mariotte's bottle filled with demineralized, de-aired water, so as to run a constant-head permeability test. Once the specimen was saturated, the position of the thin tube that goes through the Mariotte's bottle was set in such a way that the difference in height between its bottom and the top surface of the specimen represented the imposed waterhead $\Delta\Pi$ [L]. The water level in the Mariotte's bottle always had to be above the bottom of the thin tube in order to ensure a constant imposed waterhead. By measuring the water level change in the Mariotte's bottle ΔH [L] and time necessary for obtaining this change Δt [T], the flux q [L/T] can be calculated. See the following:

$$q_j = \frac{\Delta H_j}{\Delta t_j}\frac{A_{mariotte}}{A} \quad j = 1, 2, 3 \tag{2}$$

where $A_{mariotte}$ is the cross-section area [L^2] of the Mariotte's bottle, decreased by the area of the thin tube. The saturated hydraulic conductivity K_s is then calculated using Darcy's law:

$$K_{s,j} = \frac{q_j}{\Delta\Pi_j} H_{specimen} \quad j = 1, 2, 3 \tag{3}$$

The procedure was repeated for three different imposed waterheads ($j = 1, 2, 3$) that were adjusted by changing the altitude of the bottom of the thin tube.

Unsaturated States

The various existing methods of measuring the HCFs in unsaturated mediums have been described in various papers or textbooks, including those by Masrouri, Bicalho, and Kawai (2008) and Fredlund, Rahardjo, and Fredlund (2012). In steady-state methods (Corey 1957; Klute 1972; and Olsen, Nichols, and Rice 1985, among others), a constant flow is imposed in a specimen put under given values of controlled suction. These methods are known to be rather long and tedious, due in particular to the need to very precisely measure tiny transient flows along rather long periods of time. Alternatively, transient methods, in which the water outflow from the specimen submitted to suction steps is monitored (Gardner 1956; Miller and Elrick 1958; Kunze and Kirkham 1962), are known to be easier to perform, with simpler equipment (Masrouri, Bicalho, and Kawai 2008). For these reasons, transient methods were used in this work.

The HCF was hence determined by applying suction steps and monitoring the resulting changes in water content with time until equilibration by means of the differential pressure transducer. It was planned to calculate the hydraulic conductivity of the specimen by using Gardner's method (1956). This method assumes that the change in suction for each step is small in such a way that the diffusion coefficient $D(h_k)$ can reasonably be considered constant during the test:

$$D(h_k) = D = \frac{K(h_k)}{C(h_k)} = \frac{K(h_k)\Delta h_k}{\Delta\theta} \tag{4}$$

where $C(h_k)$ is the average slope of the WRC [L^{-1}] along the suction step corresponding to Δh_k [L] and $K(h_k)$ is the hydraulic conductivity [L/T]. Based on the analytical solution of the diffusion equation expressed in terms of a Fourier series, Gardner proposed an estimation of the water conductivity using the monitored volume $V(t)$ [L^3] of water extracted from the specimen:

$$V(t) = V_\infty \left(1 - \frac{8}{\pi^2} \sum_{i=1,3,5,\ldots}^{\infty} \frac{1}{i^2} e^{-\left(\frac{i}{2}\right)^2 \pi^2 \frac{t}{T}}\right) \tag{5}$$

$$T = \frac{{H_{specimen}}^2 C(h_k)}{K(h_k)} = \frac{{H_{specimen}}^2}{D} \tag{6}$$

where V_∞ is the total amount of water extracted during the suction step [L^3]. As commented earlier, we observed in this work that the specimen height $H_{specimen}$ remained reasonably constant; we hence adopted $H_{specimen} = 2.4$ cm.

Gardner's method is based on the fact that only the first member ($i = 1$) of the Fourier series in equation (5) can be taken into account as a reasonable approximate solution, acceptable after $t > t_{bound} = \frac{4{H_{specimen}}^2}{3\pi^2 D}$. In such conditions, the equation corresponding to the first member of equation (5) can be written as follows:

$$ln[V_\infty - V(t)] = ln\frac{8V_\infty}{\pi^2} - \pi^2 \frac{Dt}{4{H_{specimen}}^2} \tag{7}$$

showing that the term $ln[V_\infty - V(t)]$ becomes a linear function of time t, with a slope depending on the diffusion coefficient D.

The hydraulic conductivity $K(h_k)$ can then be calculated using the following equation:

$$K(h_k) = \frac{D\Delta\theta}{\Delta h_k} \tag{8}$$

The experimental data obtained in this work indicated that Gardner's method is more relevant at higher suctions, in which (i) less water exchanges occurred, (ii) the condition of constant suction is ensured, and (iii) the assumption about a constant diffusion coefficient D is more satisfactorily fulfilled.

However, Gardner's method cannot be directly used when the saturated hydraulic conductivity of the ceramic disk is smaller than that of the specimen. Experimental data showed that this occurred during the first steps at low suction from the saturated state, during which higher hydraulic conductivity values are obtained. To cope with the cases in which impedance effects due to the ceramic disk occur, the method proposed by Kunze and Kirkham (1962) was adopted.

Kunze and Kirkham's Method

Kunze and Kirkham (1962) considered the solution of the consolidation equation applied for various layers of soil with different hydraulic conductivities. Their solution is graphically presented through various curves showing the changes in $V(t)/V_\infty$ with respect to the variable ${\lambda_1}^2 Dt/{H_{specimen}}^2$, in which the parameter λ_1 is the first solution of equation $a\lambda_n = cot\lambda_n$ and a is the ratio between the impedance of the ceramic disk and that of the specimen.

In order to determine the hydraulic conductivity $K(h_k)$ of the specimen, it is required to estimate parameters a and λ_1, by fitting the experimental data (presented in the form $V(t) / V_\infty$ versus t) with one of the theoretical curves. Kunze and Kirkham (1962) remarked that only a portion of the experimental data corresponded to the theoretical curves, so they recommended to rather fit the curves at small times, for which more accurate values of

λ_1^2 are obtained. The choice of the adequate theoretical curve provides the value of parameter a. It is then possible to determine the corresponding parameter λ_1 from the table presented in the paper of Kunze and Kirkham (1962). It is also necessary to graphically determine the reference time t_{RP} that corresponds to $\lambda_1^2 Dt / H_{specimen}^2 = 1$. Finally, the diffusion coefficient is calculated as $D = H_{\text{specimen}}^2 / \lambda_1^2 t_{RP}$ and the hydraulic conductivity by using equation (8).

Another way to explore a possible impedance effect due to the ceramic porous disk is to apply Darcy's law to the flux going through the saturated ceramic disk as follows:

$$h_{k,top} = h_k - \Delta z_s \frac{\Delta V}{\Delta t} \frac{1}{A_{cs} K_{cs}} \tag{9}$$

where $h_{k,top}$ is the suction [L] at the top of the ceramic disk, Δz_s its thickness [L], A_{cs} its cross-section area [L^2] (7-cm diameter), and ΔV its volume [L^3] extracted from the specimen during the time interval Δt [T].

The change in suction at the top of the ceramic disk can hence be derived from the monitoring of the extracted water volume ΔV with respect to time. In the lack of any impedance effect, both suction values at top and bottom should be equal.

Experimental Results

WRC

Figure 6 shows the continuous monitoring of the changes in suction with both the hanging column technique (Steps 1 to 10) and axis translation technique (Steps 11 to 13). The outer tube was used for Steps 1 and 2 that mobilized larger water volumes (Valve V4 closed and Valve V5 opened, see fig. 5A), while the subsequent 11 steps (3–13) were made by using the inner tube (Valve V4 opened and Valve V5 closed, see fig. 5B). In the former case, the imposed suction remains constant (see fig. 7A, solid line with squares—the dashed line with triangles will be commented later on), while in the latter case (3–13), the initial instantaneous drop in height Δh_k (increase in suction) is followed by a slight progressive increase in height, corresponding to a slight decrease in suction (see for example Steps 11 and 12 in fig. 7B).

The corresponding drying path of the WRC is presented in figure 8, in which the changes in volumetric water content θ are plotted with respect to the changes in suction expressed in [kPa]. The curve evidences a significant decrease in water content for the initial steps at low suctions, with θ decreasing from the initial value of 0.395 down to 0.23 upon application of the first suction step of 2.1 kPa. The increment in volumetric water content progressively decreases afterwards, with a decrease in θ to 0.20 at a suction of 4.2 kPa. The curve finally

FIG. 6

Continuous monitoring of the imposed suctions during the 13 steps, provided by the differential pressure transducer.

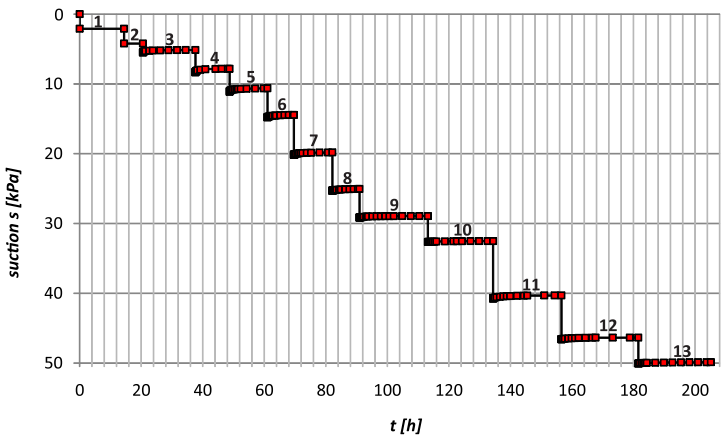

FIG. 7

Zoom of the suction changes (solid line with rectangles—imposed suction; dashed line with triangles—calculated suction at the top of the ceramic disk): (*A*) Steps 1 and 2; and (*B*) Steps 11 and 12.

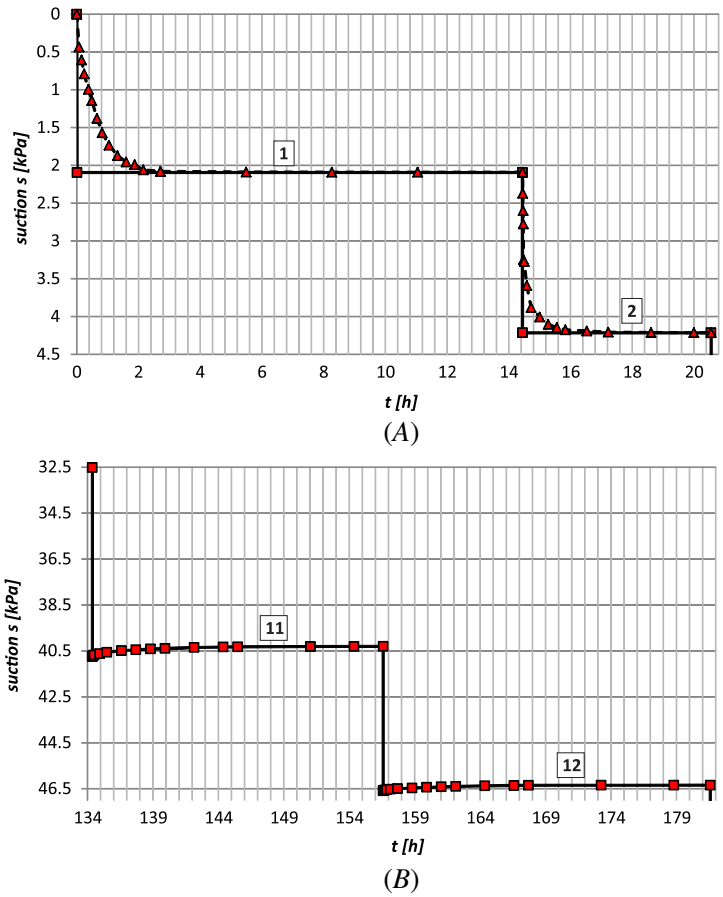

becomes almost linear at a suction larger than 14.2 kPa, indicating that the further suction increments extract small quantities of water. A final value of 0.11 is reached at 49.6 kPa. Good compatibility is observed between the section obtained with the hanging column technique (1–10) and that with the axis translation method (11–13).

Figure 8 also shows that a good fitting is obtained by using the WRC expressions of Brooks and Corey (BC; 1964) and van Genuchten (vG; 1980) as follows:

$$\text{vG}: \theta = \theta_r + \frac{\theta_s - \theta_r}{\left(1 + \left(\frac{s}{s_{ae}}\right)^n\right)^m}; \text{ with } m = 1 - \frac{1}{n} \tag{10}$$

where θ_s is the saturated volumetric water content ($\theta_s = 0.395$, see fig. 8) and θ_r [-] the residual one, s_{ae} is the air entry value of suction [M/(LT^2)], and n [-] an empirical parameter; see the following:

$$\text{BC}: \theta = \theta_r + (\theta_s - \theta_r)\left(\frac{s}{s_{ae}}\right)^{-\lambda} \tag{11}$$

where λ [-] is an empirical parameter, related to n by the relation $\lambda = n - 1$.

The fitting of the parameters of both vG and BC curves were made by first adopting values of s_{ae} and θ_r, taken equal to 0.32 kPa and 0.057, respectively. The best fitting was obtained with $n = 1.35$ (vG expression) and $\lambda = 0.35$ (BC expression).

FIG. 8

WRC obtained using both techniques of controlling suction (hanging column and axis translation).

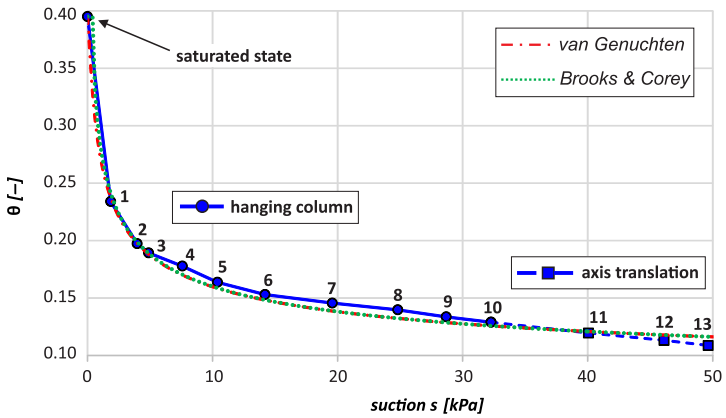

HCF

Saturated State

Figure 9 shows the data obtained from the steady-state permeability test, expressed in terms of changes in fluxes q_j with respect to the hydraulic gradient ($i = \Delta\Pi_j / H_{specimen}$, see equation (3)). The slope of the linear regression corresponding to the three measured points ($j = 1, 2, 3$) and point (0, 0) provides a value $K_s = 8.11 \times 10^{-6}$ m/s.

The same approach carried out on the ceramic porous stone provided a value $K_{cs} = 4.02 \times 10^{-8}$ m/s, confirming that the hydraulic conductivity of the saturated ceramic porous stone is significantly smaller than that of the saturated material. As a consequence, Kunze and Kirkham's method was used to interpret the data of the first suction steps (1 and 2) applied from the saturated state.

Unsaturated States

Figure 10 presents the experimental data of Steps 1 and 2 presented in terms of changes in $V(t)/V_\infty$ with respect to a log scale of $\lambda_1^2 D t_{RP}/H_{specimen}$, as proposed by Kunze and Kirkham. For Step 1, figure 10 shows excellent agreement of the data with the theoretical curve of parameter $a = 1$. The corresponding value of parameter λ_1^2 is 0.74, according to Kunze and Kirkham's (1962) graph, while the reference time t_{RP} is 47 min (2,800 s—vertical arrow in fig. 10). Finally, a hydraulic conductivity $K(s) = 2.14 \times 10^{-7}$ m/s is obtained for a suction of 2.1 kPa. This value is larger than that of the ceramic disk ($K_{cs} = 4.02 \times 10^{-8}$ m/s), confirming the necessity of accounting for the impedance effect of the porous stone.

Similarly, a value $a = 0.142$ is obtained for Step 2, with $\lambda_1^2 = 1.90$ with $t_{RP} = 24$ min (1,440 s), resulting in a hydraulic conductivity value of 3.64×10^{-8} m/s, slightly smaller than that of the ceramic porous stone.

FIG. 9

Data of the constant waterhead hydraulic conductivity measurement of the saturated material.

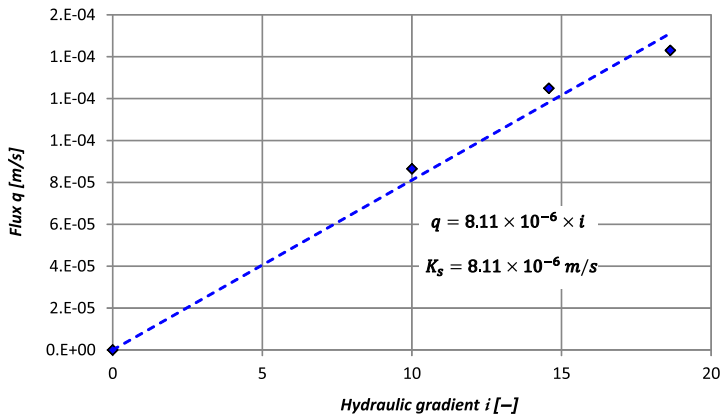

FIG. 10

Kunze and Kirkham's method applied to Steps 1 and 2 (arrow indicates t_{RP}).

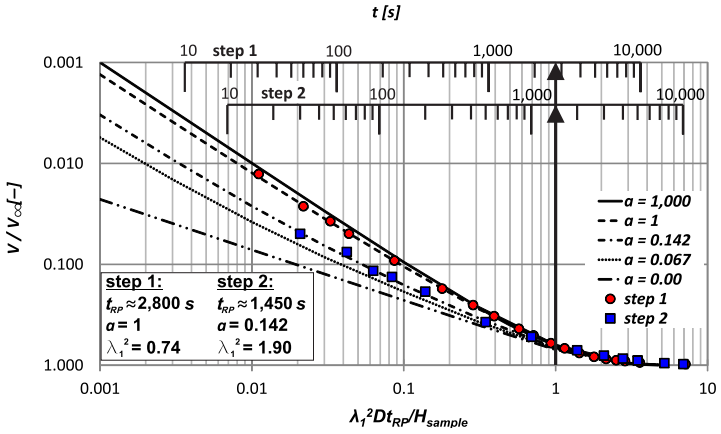

The calculations of the changes with time of the suction imposed on the top of the ceramic disk according to equation (9) are presented in **figure 7A** for Steps 1 and 2 (dashed line with triangles). As expected, they confirm the perturbation due to the low permeability of the ceramic disk. This perturbation is stronger during Step 1, in which almost 3 hours are necessary to reach the desired 2.1 kPa suction at the top, compared to Step 2, in which the 4.2 kPa imposed suction is reached at the top after less than 2 hours.

Prior to using Gardner's method, the assumption of constant suction during each suction step has to be checked. Inspection of the suction steps applied for suctions higher than 4.1 kPa (Steps 3–13, see **fig. 6**) showed that the water level in the inner tube was slightly rising at the start of the step, hence decreasing the suction. The level changes in the inner tube during Steps 3 and 4 are around 7.5 % of the imposed suction and 30 % of the imposed suction increment. These two steps do not reasonably ensure the constant suction condition; they will not be considered for the determination of the HCF. For suctions higher than 10 kPa (Measurements 5–13, see **fig. 6**), the level increase in the tube is smaller (less than 4 % of the imposed suction and less than 12 % of the imposed suction increment), and suction changes are considered to be reasonably compatible with the use of Gardner's method (see for example Steps 11 and 12 in **fig. 7B**).

The application of Gardner's method is presented in **figure 11**, which shows the changes in $ln[V_\infty - V(t)]$ with respect to time for the measurements made during Steps 2 and 5–13 (see equation (7)). In all cases, the linearity of the $ln[V_\infty - V(t)]$ function is satisfactory. As recommended by Gardner, the fitting is only based on the points corresponding to $t > t_{bound}$. The values of t_{bound}, calculated for each stage, are given in the graph of each step. Values are included between 0.2 and 2 h, depending of the value of D. Note that Step 2 was also considered here so as to compare the data with those of Kunze and Kirkham's method, which is more appropriate, given possible impedance effects.

Figure 12 shows the hydraulic conductivities obtained using the three different methods: (i) saturated hydraulic conductivity, using the constant-head permeability test; (ii) unsaturated hydraulic conductivity at lower suctions, using Kunze and Kirkham's method (Steps 1 and 2); and (iii) unsaturated hydraulic conductivity at larger suctions, using Gardner's method (Steps 2 and 5–13).

One observes that the hydraulic conductivity at Step 2 provided by Gardner's method is somewhat smaller than that (Step 2) given by Kunze and Kirkham's method. This is compatible with the impedance effect due to the low permeability of the ceramic disk, which indicates that Gardner's method is not fully satisfactory for Step 2. Note, however, that the difference in hydraulic conductivity is not that large (3.64×10^{-8} m/s for Kunze and Kirkham and 1.64×10^{-8} m/s for Gardner's method).

All the points obtained by the three methods are in reasonable agreement and provide the decrease in hydraulic conductivity with increased suction along the drying path. In the first 5 steps, a large decrease of 4 orders

FIG. 11 Data from Gardner's method, suction Steps 2 and 5–13.

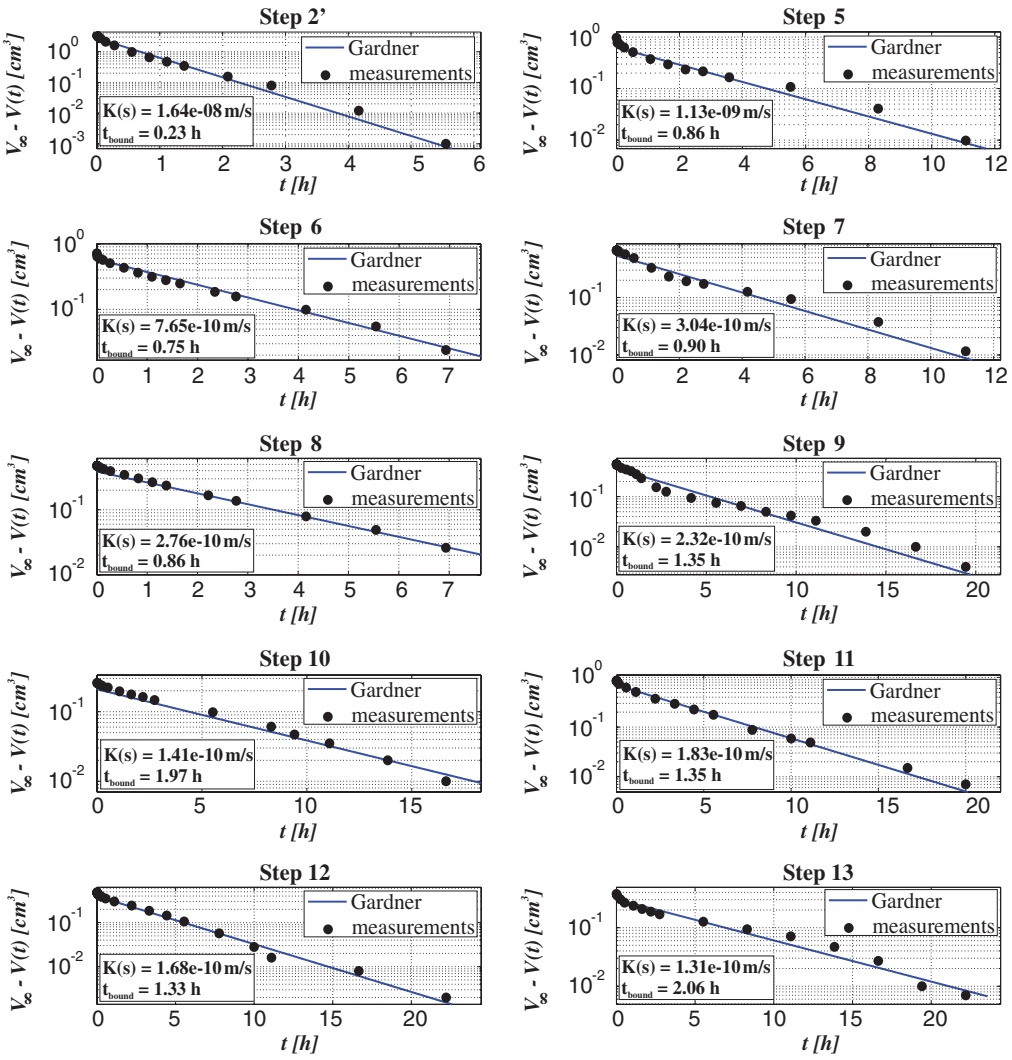

FIG. 12

HCF.

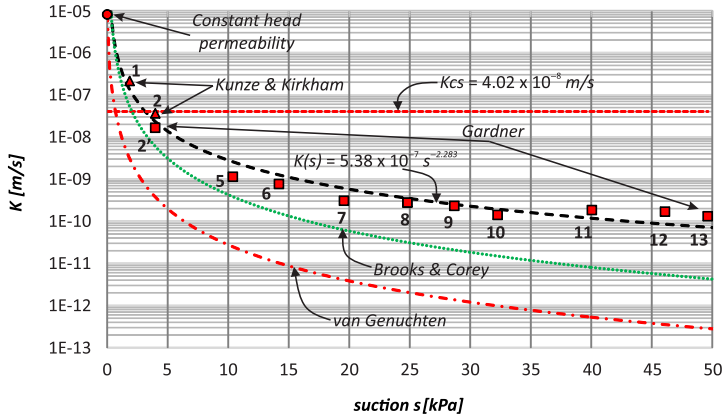

of magnitude is observed from 10^{-5} m/s (saturated state) down to 10^{-9} m/s at a suction of 10.4 kPa, and the hydraulic conductivity then stays between 10^{-9} and 10^{-10} m/s for Steps 5 to 13, corresponding to suctions between 10.4 and 49.6 kPa.

The results are also compared with the curves obtained by using the mathematical expressions of the relative hydraulic conductivity ($K_r(s) = K(s) / K_s$) derived from the WRC formulations of BC (1964) and vG (1980) according to Mualem's (1976) approach (equations (10) and (11)), as follows:

$$\text{vG}: K_r(s) = \frac{\left[1 - \left(\frac{s}{s_{ae}}\right)^{n-1}\left(1 + \left(\frac{s}{s_{ae}}\right)^{n}\right)^{-m}\right]^2}{\left(1 + \left(\frac{s}{s_{ae}}\right)^{n}\right)^{m/2}} \tag{12}$$

$$\text{BC}: K_r(s) = \left(\frac{s}{s_{ae}}\right)^{-2-5\lambda/2} \tag{13}$$

The curves obtained with the parameters obtained from the WRC curves, also represented in **figure 12**, do not satisfactorily fit with the experimental data. Both formulations underestimate the hydraulic conductivity, with a better correspondence observed with the BC formulation. Indeed, the poor performance of the vG formulation is surprising, given that both the vG and BC expressions fitted quite nicely with the WRC and that both permeability functions came through Mualem's approach. As explained earlier, the same physical parameters were adopted in both cases (air entry value s_{ae} and residual and saturated water content θ_r and θ_s, respectively), while the fitting parameters used for the WRC were n (vG) and λ (BC), also linked together ($\lambda = n - 1$). Actually, it seems that these permeability functions derived from the WRC curves are most often used in the literature without a further experimental check. A possibility could be that we deal in this work with a rather specific coarse granular material. This poor performance of the vG HCF in such a coarse material certainly deserves further attention.

Because of this poor correspondence, it was decided to propose a power law, fitted by using the root-mean-square-deviation method. This solution can be written in the following form:

$$K(s) = a_1 \times s^{b_1} \tag{14}$$

with $a_1 = 5.38$ x 10^{-7} and $b_1 = -2.283$, giving the following:

$$K(s) = 5.38 \times 10^{-7} \times s^{-2.283} \tag{15}$$

The corresponding expression of the relative permeability is then as follows:

$$\frac{K(s)}{K_s} = a_2 s^{b_1} = 6.63 \times 10^{-2} \times s^{-2.283} \tag{16}$$

In order to present the right side of equation (16) in the relative form as well, coefficient a_2 can be written as follows:

$$a_2 = \left(\frac{1}{s_{ae}}\right)^{b_1} \rightarrow s_{ae} = a_2^{-\frac{1}{b_1}} = 0.305 \tag{17}$$

where the value of s_{ae} is expressed in [kPa]. The final form of the equation reads:

$$\frac{K(s)}{K_s} = \left(\frac{s}{s_{ae}}\right)^{b} \tag{18}$$

with $s_{ae} = 0.305$ kPa and $b = b_1 = -2.283$.

Conclusion

The new device developed in this work allowed us to determine the WRC and HCF of a light coarse material used as substrate in an urban green roof. In a first estimation, it was estimated that the hanging column technique of controlling suction, with a maximum height of 3.2 m (suction 32 kPa) would have been satisfactory, but it was finally necessary to impose larger suctions by using the axis translation technique. This adaptation was rather simple to carry out, finally allowing us to run the whole test by using both techniques on the same specimen in the same cell between the saturated state and a maximum suction of 49.6 kPa, with a good comparability between the experimental data obtained by the two techniques.

The advantage of the hanging column technique is to allow for very good precision in the control of both the suction and the water exchanges, made possible by using a differential pressure sensor with an accuracy of 0.1 mm in height. A specific system based on the use of both an inner and outer tube was also developed so as to improve the accuracy of the measurements along the range of the applied suctions. This good accuracy was necessary, given the significant changes in volumetric water content observed during the first application of a suction as low as 2.1 kPa that resulted in a significant decrease from 0.40 to 0.23.

Starting from a saturated state, the WRC exhibited a drastic decrease under a small suction of 2.1 kPa, in link with the coarse nature of the granular substrate, followed by a progressive decrease down to a water content of 0.11 at 49.6 kPa. Both the vG and BC mathematical expressions fitted quite nicely with the experimental data.

The good accuracy in the measurements of suction and water exchanges also allowed us to simultaneously determine, in a simple fashion, the HCF from the monitoring of the water exchanges resulting from the step changes in suction. At lower suctions (2.1 and 4.2 kPa) and higher hydraulic conductivity, it was necessary to account for the impedance effects due to the 50-kPa air entry value ceramic disk by successfully using Kunze and Kirkham's method. Gardner's method was used at larger suctions, and a good comparability was observed from the experimental data from each technique. Another advantage of the device is to simply allow for the determination of both the WRC and HCF of the coarse material. Unsurprisingly, the HCF exhibited a trend similar to that of the WRC, with a decrease of around 3 orders of magnitude between the saturated state and that at a suction of 4.2 kPa, whereas all the data between 10.4 and 49.6 kPa were comprised between 10^{-9} and 10^{-10} m/s.

The experimental HCF data were compared with the analytical expressions derived from the WRC expressions of vG and BC, based on Mualem's approach. In both cases, these expressions appeared to significantly underestimate the experimental HCF, however with better results with BC's expression, which was less than one order of magnitude below the experimental data. These expressions of the HCF are often used in the case of a lack of experimental data, and the difference observed in this work confirms the need of operational devices for the simultaneous experimental determination of the WRC and HCF in granular materials, such as the green-roof substrate investigated in this work.

To summarize, the main advantages of the presented device are (i) its reliability for the simultaneous determination of both the WRC and HCF, thanks to the robustness and precision of both the double tube system for monitoring water exchanges, and of the high-precision differential pressure transducer for the measurement of suction; (ii) its ability to accommodate both the hanging column and axis translation techniques of controlling suction, with the largest possible suction controlled by the air entry value of the porous stone, i.e., 1,500 kPa for common ceramic porous stones; and (iii) its ability to provide relevant data within a reasonable period of time: 10 days were necessary to run 13 steps, a period that can be reduced by making less steps, resulting for instance in a time period of around 1 week for 7 steps.

Note that the technique developed in this work could be extended to larger suctions by using a ceramic disk with a larger air entry value, allowing it to reach drier states. Note however that the technique is more adapted for granular materials in which rather low suctions develop. It could exhibit some restrictions in terms of water retention properties in the case of finer soils. The range of unsaturated hydraulic permeability functions covered

during our investigation is between 10^{-5} and 10^{-10} m/s. Again, it seems that the technique would be limited, for finer soils, at larger suctions resulting in smaller HCFs.

ACKNOWLEDGMENTS

The authors are indebted to the VulkaTec Riebensahm GmbH Company (Germany) for providing the substrate material investigated in this study. They are also grateful to the two anonymous reviewers for their comments that helped improve the quality of the article.

Reference

AFNOR. 1992. *Analyse granulométrique des sols - Méthode par sédimentation*. AFNOR(1992). Paris, France: Association Française de Normalisation, approved May 20, 1992.

AFNOR. 1996. *Analyse granulométrique - Méthode par tamisage à sec après lavage*. AFNOR(1996). Paris, France: Association Française de Normalisation, approved March 5, 1996.

AFNOR. 1998. *Détermination de la teneur pondérale en matières organiques d'un matériau*. AFNOR(1998). Paris, France: Association Française de Normalisation, approved December, 1998.

ASTM International. 2006. *Standard Practice for Classification of Soils for Engineering Purposes (Unified Soil Classification System)*. ASTM D2487-06(2006). West Conshohocken, PA: ASTM International, approved May 1, 2006. https://doi.org/10.1520/D2487-06

Blatz, J. A., Y.-J. Cui, L. Oldecop. 2008. "Vapour Equilibrium and Osmotic Technique for Suction Control." *Geotechnical and Geological Engineering* 26, no. 6: 661–673. https://doi.org/10.1007/s10706-008-9196-1

Brooks, R. H. and A. T. Corey. 1964. *Hydraulic Properties of Porous Media, Hydrology Papers, no. 3*, 1–27. Fort Collins, CO: Colorado State Univeristy.

Buckingham, E. 1907. *Studies on the Movement of Soil Moisture, U. S. Department of Agriculture, Bureau of Soils, Bulletin 38*. Washington, DC: U. S. Department of Agriculture.

Corey, A.T. 1957. "Measurement of Water and Air Permeability in Unsaturated Soil." *Soil Science Society of America Journal* 21, no. 1 (January): 7–10. https://doi.org/10.2136/sssaj1957.03615995002100010003x

Delage, P. n.d. "Experimental Unsaturated Soil Mechanics: State-of-Art-Report." Paper presented at the Third International Conference on Unsaturated Soils UNSAT (Vol. 3), Recife, Brazil, March 10–13, 2002.

Delage, P. and Y.-J. Cui. 2008. "An Evaluation of the Osmotic Technique of Controlling Suction." *Geomechanics and Geoengineering: An International Journal* 3, no. 1: 1–11. https://doi.org/10.1080/17486020701868379

Esteban, F. "Caracterización de la expansividad de una roca evaporítica. Identificación de los mecanismos de hinchamiento." PhD diss., Universidad de Cantabria, 1990.

Fredlund, D. G., H. Rahardjo, and M. D. Fredlund. 2012. *Unsaturated Soil Mechanics in Engineering Practice*. Hoboken, NJ: John Wiley & Sons.

Gardner, W. R. 1956. "Calculation of Capillary Conductivity from Pressure Plate Outflow Data." *Soil Science Society of America Journal* 20, no. 3 (July): 317–320. https://doi.org/10.2136/sssaj1956.03615995002000030006x

Klute, A. 1972. "The Determination of the Hydraulic Conductivity and Diffusivity of Unsaturated Soils." *Soil Science* 113, no. 4 (April): 264–276. https://doi.org/10.1097/00010694-197204000-00006

Kunze, R. J. and D. Kirkham. 1962. "Simplified Accounting for Membrane Impedance in Capillary Conductivity Determinations." *Soil Science Society of America Journal* 26, no. 5 (September): 421–426. https://doi.org/10.2136/sssaj1962.03615995002600050006x

Masrouri, F., K. V. Bicalho, and K. Kawai. 2008. "Laboratory Hydraulic Testing in Unsaturated Soils." *Geotechnical and Geological Engineering* 26, no. 6 (December): 691–704. https://doi.org/10.1007/s10706-008-9202-7

Miller, E. E. and D. Elrick. 1958. "Dynamic Determination of Capillary Conductivity Extended for Non-Negligible Membrane Impedance." *Soil Science Society of America Journal* 22, no. 6 (November): 483–486. https://doi.org/10.2136/sssaj1958.03615995002200060002x

Mualem, Y. 1976. "A New Model for Predicting the Hydraulic Conductivity of Unsaturated Porous Media." *Water Resources Research* 12, no. 3 (June): 513–522. https://doi.org/10.1029/WR012i003p00513

Olsen, H. W., R. W. Nichols, and T. L. Rice. 1985. "Low Gradient Permeability Methods in a Triaxial System." *Géotechnique* 35, no. 2 (June): 145–157. https://doi.org/10.1680/geot.1985.35.2.145

Richards, L. A. 1941. "A Pressure-Membrane Extraction Apparatus for Soil Solution." *Soil Science* 51, no. 5 (May): 377–386. https://doi.org/10.1097/00010694-194105000-00005

Richards, L. A. 1947. "Pressure-Membrane Apparatus – Construction and Use." *Agricultural Engineering* 28: 451–460.

van Genuchten, M. Th. 1980. "A Closed-Form Equation for Predicting the Hydraulic Conductivity of Unsaturated Soils." *Soil Science Society of America Journal* 44, no. 5 (September): 892–898. https://doi.org/10.2136/sssaj1980.03615995004400050002x

Vanapalli, S. K., M. V. Nicotera, and R. S. Sharma. 2008. "Axis-Translation and Negative Water Column Techniques for Suction Control." *Geotechnical and Geological Engineering* 26 (May): 645–660. https://doi.org/10.1007/s10706-008-9206-3

Versini, P. A., A. Gires, G. Fitton, I. Tchiguirinskaia, and D. Schertzer. 2018. "Toward an Assessment of the Hydrological Components Variability in Green Infrastructures: Pilot Site of the Green Wave (Champs-sur-Marne)." *La Houille Blanche* 4 (August): 34–42. https://doi.org/10.1051/lhb/2018040

VulkaTec Riebensahm GmbH. 2016. "Vulkaplus intensiv 0/12 / Vulkaplus Intensiv Typ Leicht." http://web.archive.org/web/20190423142633/http://www.vulkatec.de/Begruenung/Dachbegruenung/Intensivbegruenung-bei-Substratstaerken-bis-50cm/Vulkaplus-Intensiv-0_12/?&d=1

Zur, B. 1966. "Osmotic Control the Matric Soil-Water Potential: I. Soil-Water System." *Soil Science* 102, no. 6 (December): 394–398. https://doi.org/10.1097/00010694-196612000-00007

Copyright by ASTM International (all rights reserved), pursuant to License Agreement. No further reproduction authorized.